Integrated network pharmacology and molecular docking approaches to reveal the synergistic mechanism of multiple components in *Venenum Bufonis* for ameliorating heart failure

Wei Ren [1], **Zhiqiang Luo** [2], **Fulu Pan** [3], **Jiali Liu** [1], **Qin Sun** [1], **Gang Luo** [1], **Raoqiong Wang** [1], **Haiyu Zhao** [4], **Baolin Bian** [4], **Xiao Xiao** [5], **Qingrong Pu** [1], **Sijin Yang** [Corresp., 1], **Guohua Yu** [Corresp. 2]

[1] Affiliated Traditional Chinese Medicine Hospital, Southwest Medical University, Luzhou, China

[2] School of Life Sciences, Beijing University of Chinese Medicine, Beijing, China

[3] School of Chinese Materia Medica, Beijing University of Chinese Medicine, Beijing, China

[4] Institute of Chinese Materia Medica, China Academy of Chinese Medical Sciences, Beijing, China

[5] Beijing National Laboratory for Molecular Sciences, Key Laboratory of Analytical Chemistry for Living Biosystems, CAS Research/Education Center for Excellence in Molecular Sciences, Institute of Chemistry, Chinese Academy of Sciences, Beijing, China

Corresponding Authors: Sijin Yang, Guohua Yu
Email address: ysjimn@sina.com, 202002016@bucm.edu.cn

Venenum Bufonis (VB), also called Chan Su in China, has been extensively used as a traditional Chinese medicine (TCM) for treating heart failure (HF) since ancient time. However, the active components and the potential anti-HF mechanism of VB remain unclear. In the current study, the major absorbed components and metabolites of VB after oral administration in rats were first collected from literatures. A total of 17 prototypes and 25 metabolites were gathered. Next, a feasible network-based pharmacological approach was developed and employed to explore the therapeutic mechanism of VB on HF based on the collected constituents. In total, 158 main targets were screened out and considered as effective players in ameliorating HF. Then, the VB components–main HF putative targets–main pathways network was established, clarifying the underlying biological process of VB on HF. More importantly, the main hubs were found to be highly enriched in adrenergic signalling in cardio-myocytes. After verified by molecular docking studies, four key targets (ATP1A1, GNAS, MAPK1 and PRKCA) and three potential active leading compounds (bufotalin, cinobufaginol and 19-oxo-bufalin) were identified, which may play critical roles in cardiac muscle contraction. This study demonstrated that the integrated strategy based on network pharmacology and molecular docking was helpful to uncover the synergistic mechanism of multiple constituents in TCM.

1 **Integrated network pharmacology and molecular docking approaches to**

2 **reveal the synergistic mechanism of multiple components in *Venenum Bufonis***

3 **for ameliorating heart failure**

4 Wei Ren*[1], Zhiqiang Luo*[2], Fulu Pan*[3], Jiali Liu[1], Qin Sun[1], Gang Luo[1], Raoqiong Wang[1],

5 Haiyu Zhao[4], Baolin Bian[4], Xiao Xiao[5], Qingrong Pu[1], Sijin Yang[1] and Guohua Yu[2]

6 [1] Affiliated Traditional Chinese Medicine Hospital, Southwest Medical University, Luzhou

7 646000, China

8 [2] School of Life Sciences, Beijing University of Chinese Medicine, Beijing 102488, China

9 [3] School of Chinese Materia Medica, Beijing University of Chinese Medicine, Beijing 102488,

10 China

11 [4] Institute of Chinese Materia Medica, China Academy of Chinese Medical Sciences, Beijing

12 100700, China

13 [5] Beijing National Laboratory for Molecular Sciences, Key Laboratory of Analytical Chemistry

14 for Living Biosystems, CAS Research/Education Center for Excellence in Molecular Sciences,

15 Institute of Chemistry, Chinese Academy of Sciences, Beijing 100190, China

16 Corresponding Author:

17 Sijin Yang[1], Guohua Yu[2]

18 [1]Affiliated Traditional Chinese Medicine Hospital, Southwest Medical University, No.182

19 Chunhui Road, Longmatan District, Luzhou 646000, Sichuan Province, China.

20 [2]School of Life Sciences, Beijing University of Chinese Medicine, the northeast corner of the

21 intersection of yangguang south street and baiyang east road, Fangshan District, Beijing 102488,

22 China.

23 E-mail addresses: ysjimn@sina.com (S. Yang); 202002016@bucm.edu.cn (G. Yu)

24 *These authors contributed equally.

25 **Abstract**

26 *Venenum Bufonis* (VB), also called Chan Su in China, has been extensively used as a

27 traditional Chinese medicine (TCM) for treating heart failure (HF) since ancient time. However,

28 the active components and the potential anti-HF mechanism of VB remain unclear. In the current

29 study, the major absorbed components and metabolites of VB after oral administration in rats

30 were first collected from literatures. A total of 17 prototypes and 25 metabolites were gathered.

31 Next, a feasible network-based pharmacological approach was developed and employed to

32 explore the therapeutic mechanism of VB on HF based on the collected constituents. In total, 158

33 main targets were screened out and considered as effective players in ameliorating HF. Then, the

34 VB components–main HF putative targets–main pathways network was established, clarifying

35 the underlying biological process of VB on HF. More importantly, the main hubs were found to

36 be highly enriched in adrenergic signalling in cardio-myocytes. After verified by molecular

37 docking studies, four key targets (ATP1A1, GNAS, MAPK1 and PRKCA) and three potential

38 active leading compounds (bufotalin, cinobufaginol and 19-oxo-bufalin) were identified, which

39 may play critical roles in cardiac muscle contraction. This study demonstrated that the integrated

40 strategy based on network pharmacology and molecular docking was helpful to uncover the

41 synergistic mechanism of multiple constituents in TCM.

42 **Keywords:** *Venenum Bufonis*, heart failure, network pharmacology, molecular docking

43 **1. Introduction**

44   Heart failure (HF), a multifactorial degenerative disease, occurs when the heart is not able

45   to pump blood efficiently to satisfy the oxygen and nutritional needs of the body (Asano et al.

46   2019). HF affects over 26 million people worldwide and continues to represent a major burden

47   for public health due to its high mortality, morbidity and healthcare expenses (Di Palo & Barone

48   2020; Lother & Hein 2016). The incidence rate of HF rises in magnitude with age and the major

49   etiologies were coronary heart disease, abnormal heart valves and hypertension (Akkineni et al.

50   2019). Western medicines, such as angiotensin converting enzyme (ACE) inhibitors, diuretics, β-

51   adrenergic blockers, angiotensin receptor I antagonists and positive inotropic agents, are

52   currently the main treatment programs for HF (Xu et al. 2020; Yang et al. 2020). However, long-

53   term use of these chemical drugs will lead to a series of adverse reactions like electrolyte

54   depletion, fluid depletion, and hypotension (Jia et al. 2020). Therefore, novel alternative or

55   synergetic anti-HF therapies are greatly needed.

56   *Venenum Bufonis* (VB) is the dried white secretion of the auricular and skin glands of *Bufo*

57   *bufo gargarizans* Cantor or *Bufo melanostictus* Schneider (He et al. 2019; Yun et al. 2009). As a

58   precious traditional Chinese medicine (TCM), VB has long been used for treating heart failure,

59   arrhythmia, swells, sore throat, pains, cancers and many other diseases (Liang et al. 2008; Pan et

60   al. 2020). Extensive natural product studies have indicated that VB contains a high level of

61   bufadienolides and many other constituents like alkaloids, cyclic amides, sterols, polypeptides,

62   proteins, polysaccharides, and organic acids (Wei et al. 2019). Modern pharmacological studies

63   have confirmed that VB exhibited a variety of pharmacological effects, including cardiotonic,

64   antinociceptive, anti-tumor, anesthetic, anti-inflammatory as well as antimicrobial properties

65   (Wei et al. 2020). Importantly, it is evident that VB exerts a strong cardiac excitatory effect like

66   that of digitalis, and the drug possesses many advantages such as no accumulation, quick-acting

67   and diuretic action (Wei et al. 2019). According to the Chinese Pharmacopoeia (2015 edition),

68   VB is contained in many TCM prescriptions for the treatment of HD, such as Jiuxin Pill and

69   Shexiang Baoxin Pill (Chinese Pharmacopoeia Commission, 2015). Although well-practiced in

70   clinical medicine, the holistic pharmacological mechanisms of VB on HF are largely unknown.

71   As an emerging field of pharmacology, network pharmacology delivers a systematic and

72   holistic understanding of drug action and disease complexity, which shares key ideas with the

73   integrality and systematicness of TCM theory (Luo et al. 2020; Zhang et al. 2020). An increasing

74   body of evidence suggests that network pharmacology is a powerful tool to illuminate the

75   integration synergistic mechanism of action of TCM from the multi-dimensional perspective

76   (Chen et al. 2019; Miao et al. 2019). For example, the bioactive candidates and underlying

77   mechanisms of *Cichorium glandulosum* for ameliorating type 2 diabetes mellitus was

78   successfully elucidated using "compound–target" network analysis (Qin et al. 2019). The action

79   mechanism of *Carthamus tinctorius* L. on cardiovascular disease was also elaborated based on

80   the "compound-protein/gene-disease" network (Yu et al. 2019). However, due to the limitation

81   of this method, many previous researches usually collected TCM components from related TCM

82   databases to establish the compound–target map. The candidate compounds might not be in line

83   with the components actually delivered into the blood circulatory system, which unavoidably

84   produced unreal results (Ding et al. 2019; Zhang et al. 2018).

85   In this study, first the *in vivo* ingredients of VB after oral administration in rats were taken

86   from the literature. Second, the VB- and HF-associated targets were predicted. Third, network

87 construction and pathway enrichment analysis were used to explore the active components and

88 the potential targets relevant to the treatment of HF with VB. Finally, molecular docking was

89 performed to confirm the specific interactions between VB and the candidate targets. The above

90 study not only provides a comprehensive understanding about the molecular mechanism of VB

91 acting on HF, but also offers a rapid and effective strategy for screening desired compounds from

92 TCM. The flowchart was illustrated in Fig. 1.

93 **2.   Materials and methods**

94 2.1. *In vivo* constituents of VB

95   A total of 42 *in vivo* constituents of VB have been reported, including 17 prototypes and 25

96   metabolites (He et al. 2012; Liang et al. 2008; Miyashiro et al. 2008; Ning et al. 2010; Tao et al.

97   2017; Xia et al. 2010; Xin et al. 2016; Zhu et al. 2013). The molecular 2D files of these

98   constituents were downloaded from the ChemSpider database (http://www.chemspider.com/) and

99   were saved in mol format (step 1 in Fig. S1). The details were listed in Table S1.

100 2.2. The prediction of VB-related targets

101   The predicted proteins targeted by the *in vivo* constituents of VB were screened from

102 MedChem Studio (MedChem Studio, 3.0; Simulations Plus, Inc, Lancaster, CA, USA, 2012).

103 This software could efficiently capture the FDA-approved drugs that have similar chemical

104 structures to the components in TCM (Yu et al. 2016). We picked out VB compound-drug pairs

105 with high confidence scores ($\geq$0.6) and considered the target proteins of the known drugs as the

106 VB-related targets. Other parameters were set as the default values (step 1 in Fig. S1).

107 2.3. Known therapeutic targets for HF

108   In this study, two databases were employed in acquiring pathological targets for HF, by use

109 of "heart failure" as the query. One was the DrugBank database (http://www.drugbank.ca/,

110 version 5.1.1), which could provide detailed information on the drug targets and their links with

111 human diseases (Griesenauer et al. 2019). Only drug–target interactions for FDA-approved anti-

112 HF drugs and potential human protein targets associated with HF were selected for further

113 analysis. The second platform was the Online Mendelian Inheritance in Man (OMIM) database

114 (http://www.omim.org/, updated on May 4, 2018), a constantly updated database of human

115 genetic diseases and genes (step 1 in Fig. S1) (Hamosh et al. 2005).

116 2.4. Protein–protein interaction (PPI) data

117   The PPI information related to the putative targets of VB constituents and known

118 therapeutic targets for HF was harvested by use of STRING (Search Tool for the Retrieval of

119 Interacting Genes/Proteins) database (http://string-db.org/). This database could provide a global

120 perspective of proteins and their functional interactions and associations (Jensen et al. 2009).

121 Results were limited to "*Homo sapiens*" and protein interactions with a confidence score greater

122 than or equal to 0.4 would be selected. Other parameters were set as the default values (step 2 in

123 Fig. S1).

124 2.5. Network construction and analysis

125   In order to illustrate the interaction among the ingredients, targets and diseases, a

126 "ingredient–target–disease" network was built by introducing the information of candidate

127 compounds of VB, putative targets of VB and HF-associated targets into Cytoscape software

128   (version 3.6.0, Boston, MA, USA). This software is an efficient open source bioinformatics tool

129   for visualizing and analysing the complex biological networks (Shannon et al. 2003). Three

130   important topological characteristics ("degree", "betweenness", and "closeness"), which have

131   been described in our previous publication (Yu et al. 2018), were calculated to assess the central

132   attribute of each hub node in the network by use of the Cytoscape plugin "Network Analyzer".

133   And "degree" > median degree centrality, "betweenness" > median betweenness centrality and

134   "closeness" > median closeness centrality were adopted as the screening criteria to acquire the

135   critical targets (Luo et al. 2020). Other parameters were set as the default values (step 2 in Fig.

136   S1).

137   2.6. Pathway enrichment analysis

138   Kyoto Encyclopedia of Genes and Genomes (KEGG) pathways analysis and Gene

139   Ontology (GO) enrichment analysis were undertaken to explore the potential functions of the

140   pivotal target proteins involved in the VB-mediated treatment of HF(Nguyen et al. 2019a,

141   Nguyen et al. 2019b), by use of the Database for Annotation, Visualization and Integrated

142   Discovery (DAVID) system (http://david.abcc.ncifcrf.gov/home.jsp/, v6.8) (Dennis et al. 2003).

143   Relevant pathways with the false discovery rate (FDR)-corrected P-value < 0.05 were considered

144   statistically significant. Other parameters were set as the default values (step 3 in Fig. S1).

145   2.7. Molecular docking simulation

146   Molecular docking studies were conducted to further verify the reliability of the potential

147   targets using CDOCKER module implemented in Discovery Studio 2016 (DS 2016).

148   CDOCKER is a semi-flexible molecular docking analysis method based on the CHARMm force

149 field, which can produce high-precision docking results, and it provides information on the

150 interaction binding energy and ligand–receptor docking mode. The three-dimensional (3D)

151 structures of the candidate compounds were generated using Chem3D Pro 12.0 and the

152 crystallographic structures of the proteins encoded by the candidate target genes were obtained

153 from the PDB database (http://www.rcsb.org/pdb/home/home.do), which was then decorated by

154 removing the ligands, adding hydrogen, removing water, optimizing and patching amino acids.

155 The binding site was defined by the ligand atoms, and the radius range was automatically

156 generated. After each compound was docked, the 10 best conformations were obtained (Yang,

157 2020). Finally, CDOCKER interaction energies (CIEs) were used to assess the binding affinities

158 between the core targets and the corresponding compounds. And the conformation corresponding

159 to the lowest CIE was selected as the most probable binding conformation. All parameters used

160 in calculation were default except for explained (step 4 in Fig. S1).

161 **3. Results and discussion**

162 3.1. Putative targets for VB

163   As shown in Table S2, a total of 260 potential targets of the *in vivo* components of VB were

164 obtained by MedChem Studio. The results showed that the candidate compounds could act on

165 multiple targets, and one target could also be linked to multiple components.

166 3.2. Known therapeutic targets for HF

167   We collected 109 and 199 HF-related targets from DrugBank database and OMIM database,

168 respectively. We then checked the data and eliminate redundant entries, leaving a final dataset of

169 292 targets associated with HF (Table S3). Among them, 22 targets were both the VB- and HF-

170 related targets, including NR1I2, MT-CO1, CA2, NR3C1, SHBG, ATP1A1, CYP17A1, PGR,

171 NR3C2, MME, AR, ACE, PRKCA, CYP11B2, RXRA, PPARG, PIK3CG, PPARD, PDE4B,

172 KCNMA1, MED1 and HIF1A.

173 3.3. Network and pathway analysis

174   To facilitate scientific interpretation of the complex relationships between VB and HF, a

175 "chemical target-disease associated gene" network, comprising the VB-related targets and the

176 HF-related targets, was constructed based on the PPI data from STRING database. As listed in

177 Table S4, this network was composed of 461 nodes and 5009 edges. After computing the values

178 of the topological features of all hubs, 158 major hubs were identified because they satisfied the

179 criteria (degree cutoff =19, betweenness cutoff = 0.001659, and closeness cutoff = 0.381426).

180 Among them, 93 hubs were VB-related targets, 65 hubs were HF-related targets. These major

181 hubs may play a critical role in the entire interaction network. The specific information about the

182 major hubs was shown in Table S5.

183 3.4. Potential mechanisms of VB in treating HF

184   To elucidate the biological process (BP), molecular function (MF), cellular components

185 (CC) of these major hubs involved in, GO enrichment analysis was conducted on the major hubs.

186 As shown in Fig. 2a-c, the top 10 significant GO entries ($P < 0.05$) were selected on the basis of

187 P value.

188   To deeply determine the function and systemic association of the main hubs, KEGG

189 pathway enrichment analysis were conducted. The results indicated that these hubs were

190 enriched in 101 significant pathways ($P < 0.05$). As shown in Fig. 2d, the top 11 pathways were

191 considered as the main biological processes involved in the treatment. To further identify the

192 functional mechanisms of VB on HF, the candidate compounds-main VB-related targets-main

193 pathways network diagram was generated and elucidated in Fig. 3. The hubs can be mainly

194 divided into the following three functional modules (circles): signal transduction (including

195 adrenergic signalling in cardio-myocytes, calcium signalling pathway, cAMP signalling

196 pathway, dilated cardiomyopathy, long-term potentiation and cGMP-PKG signalling pathway),

197 cardiovascular system (including cardiac muscle contraction, vascular smooth muscle

198 contraction and hypertrophic cardiomyopathy), and neural regulation (including dopaminergic

199 synapse and circadian entrainment). Interestingly, adrenergic signalling in cardio-myocytes was

200 highly enriched in KEGG pathway analysis, which played a critical role in the regulation of

201 cardiac muscle contraction (the top-ranked GO: Biological Process terms), suggesting that VB

202 may impart therapeutic effects on HF majorly through adrenergic signalling in cardio-myocytes.

203   As shown in Table S6, the VB putative targets associated with adrenergic signalling in

204 cardio-myocytes include guanine nucleotide-binding protein G(s) subunit alpha (GNAS),

205 adenylate cyclase 2 (ADCY2), ADCY5, protein phosphatase 1 catalytic subunit gamma

206 (PPP1CC), protein phosphatase 2 catalytic subunit alpha (PPP2CA), protein phosphatase 2

207 catalytic subunit beta (PPP2CB), calcium voltage-gated channel subunit alpha1 C (CACNA1C),

208 CACNA1D, ATPase Na^+/K^+ transporting subunit alpha 1 (ATP1A1), mitogen-activated protein

209 kinase 1 (MAPK1), protein kinase C alpha (PKCα, encoded by PRKCA). Fig. 4 depicts a

210 graphical overview of adrenergic signalling in cardio-myocytes influenced by main putative

211 targets of VB components.

212   3.5. Molecular docking

213   Table 1 displayed the CIEs (top 5 for each target) of VB hit constituents against the active

214   sites of the screened targets in adrenergic signalling, including ATP1A1, GNAS, ADCY2,

215   ADCY5, PPP1CC, PPP2CA, PPP2CB, CACNA1C, CACNA1D, MAPK1 and PRKCA. The

216   results indicated that the VB-related components had been docked successfully with ATP1A1,

217   GNAS, MAPK1 and PRKCA, which may be the key targets involved in VB for the treatment of

218   HF. Herein, we selected four representative pairs of binding interactions to illustrate how the

219   four targets bound to their corresponding components (Fig. 5). The interplay between ATP1A1

220   and bufotalin was depicted in Fig. 5a and Fig. 5b. The hydroxyl groups on bufotalin could form

221   three hydrogen bonds with SER209, ARG191 and VAL712. Another key residue which involved

222   in interaction was MET157. The binding mode of GNAS and cinobufaginol was depicted in Fig.

223   5c and Fig. 5d. The hydroxyl groups could bind with LEU171, MET255, ASN254 and LYS300

224   by forming hydrogen bonds. The carbonyl on the lactone ring could also form hydrogen bond

225   with LYS305. In addition, the lactone ring could bind with GLU164 and LYS305 via pi-anion

226   and pi-cation interactions. Other interactions including alkyl and pi-alkyl were connected with

227   ALA303, TYR163 and LEU296. The action mode of MAPK1 and cinobufaginol was depicted in

228   Fig. 5e and Fig. 5f. Cinobufaginol could form five hydrogen bonds with LYS112, LYS52 and

229   TYR34. In addition, the lactone ring could bind with ASP109 via pi-anion interaction. Other

230   interactions including alkyl and pi-alkyl were connected with VAL37. The interplay between

231   PRKCA and 19-oxo-bufalin was depicted in Fig. 5g and Fig. 5h. The hydroxyl groups of 19-oxo-

232   bufalin could form two hydrogen bonds with PRO202 and LYS230. Another key residue which

233 involved in interaction was LEU200.

234 **4. Discussion**

235   Many pathways are involved in adrenergic signalling for the regulation of cardiac

236 contractile function. Among them, the best described is the mechanism mediated by β-adrenergic

237 receptor (β-AR)–Gs–adenylate cyclase (AC) pathway (Baker 2014). Activation of β-AR–Gs–AC

238 plays an important role in increasing heart rate and force of myocardial contraction (Chen et al.

239 2020; Santulli & Iaccarino 2016). According to our predicted results, VB could regulate β-AR–

240 Gs–AC pathway by targeting Gs (GNAS) and AC (ADCY2 and ADCY5). The regulation of

241 Ca^{2+} homeostasis is also important for the cardio-myocyte excitation and cardiac electrical

242 activity (Arakelyan et al. 2007). According to our predicted results, VB could regulate cardiac

243 Ca^{2+} cycling by targeting PP1 (PPP1CC), PP2A (PPP2CA, PPP2CB), and LTCC (CACNA1C,

244 CACNA1D). Na^+/K^+-ATPase, a ubiquitous membrane protein composed of two subunits

245 denoted as α and β, is also a critical regulator in maintaining the balance of Ca^{2+} in cardio-

246 myocytes (Orlov et al. 2020; Šeflová et al. 2017). An increasing body of evidence suggests that

247 bufadienolides in VB possess inhibition effects on Na^+/K^+-ATPase (Orlov et al. 2020; Sousa et

248 al. 2017), such as bufalin (Lan et al. 2018; Laursen et al. 2015), cinobufagin (Wang et al. 2014),

249 marinobufagenin (Strauss et al. 2019), arenobufagin (Cruz Jdos & Matsuda 1993), and

250 hellebrigenin (Moreno et al. 2013). Therefore, the cardiotonic effect of VB may be mainly

251 through the suppression of Na^+/K^+-ATPase. Inhibition of the Ca^{2+}/PKCα/ERK1/2 signal pathway

252 plays a significant role in attenuating the progression of heart failure (Braz et al. 2004; Molkentin

253 & Robbins 2009). Several components from VB have been reported to inhibit the activity PKCα

254   and ERK, such as bufalin (Wu et al. 2015), marinobufagin (Bagrov et al. 2000; Fedorova et al.

255   2003) and cinobufagin (Baek et al. 2015).

256   Based on the data analysis above, the bufadienolides may be the main active components in

257   VB, which exert anti-HF effects via synergistically acting on multiple targets in multiple

258   pathways. Among them, the positive inotropic effect of VB produced through the inhibition of

259   Na^+/K^+-ATPase has been demonstrated in many basic researches and clinical practices. The

260   molecular docking results indicated that the representative compounds could connect with the

261   active-site residues via various noncovalent interactions, including the hydrogen bonding, pi-

262   alkyl, pi-anion and pi-cation, etc, which was valuable for understanding of the action

263   mechanisms of VB. In addition, according to -CIE values, bufotalin, cinobufaginol and 19-oxo-

264   bufalin showed the best performance and thus were considered as the potential active leading

265   compounds of the corresponding targets. Further researches on other potential targets or

266   pathways are required to validate the predicted results.

267   **5. Conclusion**

268   In summary, the active components of VB and their synergistic mechanisms for alleviating

269   HF were successfully unveiled by network pharmacology coupled with molecular docking

270   approach. The adrenergic signaling involved in cardiac muscle contraction process was found to

271   be mainly responsible for the anti-HF effect of VB *in silico*. Four core targets and their

272   corresponding leading compounds were identified, which may provide valuable information for

273   further experimental validations and drug discovery.

274 **Additional information and declarations**

275 **Acknowledgements**

276 This work was supported by the National Traditional Chinese Medicine Clinical Research Base
277 (Grant NO. [2020]33).

278 **Competing interests**

279 The authors declare that there are no competing interests.

280 **Author contributions**

281 Wei Ren performed the experiments, wrote the paper, approved the final manuscript.

282 Zhiqiang Luo performed the experiments, wrote the paper, approved the final manuscript.

283 Fulu Pan performed the experiments and wrote the paper, approved the final manuscript.

284 Jiali Liu analyzed the data, approved the final manuscript.

285 Qin Sun analyzed the data, approved the final manuscript.

286 Gang Luo prepared figures and/or tables, approved the final manuscript.

287 Raoqiong Wang prepared figures and/or tables, approved the final manuscript.

288 Haiyu Zhao provide software, approved the final manuscript.

289 Baolin Bian provide software, approved the final manuscript.

290 Xiao Xiao reviewed drafts of the manuscript, approved the final manuscript.

291 Qingrong Pu reviewed drafts of the manuscript, approved the final manuscript.

292 Sijin Yang conceived and designed the experiments, approved the final manuscript.

293 Guohua Yu conceived and designed the experiments, approved the final manuscript.

294 **Data availability**

295 The following information was supplied regarding data availability:

296 The raw measurements are available in the Supplemental Files.

297 **Supplemental information**

298 Supplemental information for this article can be found online at http://

299 **References**

300 **Akkineni S, Mohammed O, Pathiraj J, Devasia T, Chandrababu R, and Kunhikatta V.**

301 **2019.** Readmissions and clinical outcomes in heart failure patients: A retrospective study.

302 *Clinical Epidemiology and Global Health.* https://doi.org/10.1016/j.cegh.2019.11.002

303 **Arakelyan KP, Sahakyan YA, Hayrapetyan LR, Khudaverdyan DN, Ingelman-Sundberg**

304 **M, Mkrtchian S, and Ter-Markosyan AS. 2007.** Calcium-regulating peptide hormones

305 and blood electrolytic balance in chronic heart failure. *Regulatory Peptides* **142(3)**:95-

306 100. https://doi.org/10.1016/j.regpep.2007.02.001

307 **Asano R, Abshire M, Dennison-Himmelfarb C, and Davidson PM. 2019.** Barriers and

308 facilitators to a 'good death' in heart failure: An integrative review. *Collegian* **26(6)**:651-

309 665. https://doi.org/10.1016/j.colegn.2019.09.010

310 **Baek SH, Kim C, Lee JH, Nam D, Lee J, Lee SG, Chung WS, Jang HJ, Kim SH, and Ahn**

311 **KS. 2015.** Cinobufagin exerts anti-proliferative and pro-apoptotic effects through the

312 modulation ROS-mediated MAPKs signaling pathway. *Immunopharmacology and*

313 *Immunotoxicology* **37(3)**:265-273. DOI 10.3109/08923973.2015.1027916

314 **Bagrov AY, Dmitrieva RI, Dorofeeva NA, Fedorova OV, Lopatin DA, Lakatta EG, and**

315   **Droy-Lefaix MT. 2000.** Cicletanine reverses vasoconstriction induced by the

316   endogenous sodium pump ligand, marinobufagenin, via a protein kinase C dependent

317   mechanism. *Journal of Hypertension* **18(2)**:209-215. DOI 10.1097/00004872-

318   200018020-00012

319   **Baker AJ. 2014.** Adrenergic signaling in heart failure: a balance of toxic and protective effects.

320   *Pflugers Archiv : European journal of physiology* **466(6)**:1139-1150. DOI

321   10.1007/s00424-014-1491-5

322

323   **Braz JC, Gregory K, Pathak A, Zhao W, Sahin B, Klevitsky R, Kimball TF, Lorenz JN,**

324   **Nairn AC, Liggett SB, Bodi I, Wang S, Schwartz A, Lakatta EG, DePaoli-Roach**

325   **AA, Robbins J, Hewett TE, Bibb JA, Westfall MV, Kranias EG, and Molkentin JD.**

326   **2004.** PKC-α regulates cardiac contractility and propensity toward heart failure. *Nature*

327   *Medicine* **10(3)**:248-254. DOI 10.1038/nm1000

328   **Chen JJ, Marsden AN, Scott CA, Akimzhanov AM, and Boehning D. 2020.** DHHC5

329   Mediates β-Adrenergic Signaling in Cardiomyocytes by Targeting Gα Proteins.

330   *Biophysical Journal* **118(4)**:826-835. https://doi.org/10.1016/j.bpj.2019.08.018

331   **Chen S, Guo W, Qi X, Zhou J, Liu Z, and Cheng Y. 2019.** Natural alkaloids from lotus

332   plumule ameliorate lipopolysaccharide-induced depression-like behavior: integrating

333   network pharmacology and molecular mechanism evaluation. *Food & Function*

334   **10(9)**:6062-6073. DOI 10.1039/c9fo01092k

335   **Chinese Pharmacopoeia Commission. 2015.** *Pharmacopoeia of People's Republic of China*

336   *Part I..* Beijing: People's Medical Publishing House.

337   **Cruz Jdos S, and Matsuda H. 1993.** Arenobufagin, a compound in toad venom, blocks Na(+)-

338   K+ pump current in cardiac myocytes. *European Journal of Pharmacology* **239(1-3)**:223-

339   226. DOI 10.1016/0014-2999(93)90999-x

340   **Dennis G, Jr., Sherman BT, Hosack DA, Yang J, Gao W, Lane HC, and Lempicki RA.**

341   **2003.** DAVID: Database for Annotation, Visualization, and Integrated Discovery.

342   *Genome Biology* **4(5)**:P3-P3.

343   **Di Palo KE, and Barone NJ. 2020.** Hypertension and Heart Failure: Prevention, Targets, and

344   Treatment. *Heart Failure Clinics* **16(1)**:99-106. https://doi.org/10.1016/j.hfc.2019.09.001

345   **Ding M, Ma W, Wang X, Chen S, Zou S, Wei J, Yang Y, Li J, Yang X, Wang H, Li Y,**

346   **Wang Q, Mao H, Gao X, and Chang Y. 2019.** A network pharmacology integrated

347   pharmacokinetics strategy for uncovering pharmacological mechanism of compounds

348   absorbed into the blood of Dan-Lou tablet on coronary heart disease. *Journal of*

349   *Ethnopharmacology* **242**:112055. https://doi.org/10.1016/j.jep.2019.112055

350   **Dobrev D, and Wehrens XHT. 2010.** Calmodulin Kinase II, Sarcoplasmic Reticulum Ca2+

351   Leak, and Atrial Fibrillation. *Trends in Cardiovascular Medicine* **20(1)**:30-34.

352   https://doi.org/10.1016/j.tcm.2010.03.004

353   **Fedorova OV, Talan MI, Agalakova NI, Droy-Lefaix MT, Lakatta EG, and Bagrov AY.**

354   **2003.** Myocardial PKC beta2 and the sensitivity of Na/K-ATPase to marinobufagenin are

355   reduced by cicletanine in Dahl hypertension. *Hypertension* **41(3)**:505-511. DOI

356   10.1161/01.Hyp.0000053446.43894.9f

Manuscript to be reviewed

357 **Griesenauer RH, Schillebeeckx C, and Kinch MS. 2019.** Assessing the public landscape of

358   clinical-stage pharmaceuticals through freely available online databases. *Drug Discovery*

359   *Today* **24(4)**:1010-1016. DOI 10.1016/j.drudis.2019.01.010

360 **Hamosh A, Scott AF, Amberger JS, Bocchini CA, and McKusick VA. 2005.** Online

361   Mendelian Inheritance in Man (OMIM), a knowledgebase of human genes and genetic

362   disorders. *Nucleic Acids Research* **33**:D514-D517. DOI 10.1093/nar/gki033

363 **He R, Ma H, Zhou J, Zhu Z, Lv X, Li Q, Wang H, Yan Y, Luo N, Di L, Wu Q, and Duan J.**

364   **2019.** High Resolution Mass Profile of Bufadienolides and Peptides Combing with Anti-

365   Tumor Cell Screening and Multivariate Analysis for the Quality Evaluation of Bufonis

366   Venenum. *Molecules (Basel, Switzerland)* **24(10)**:1943. DOI

367   10.3390/molecules24101943

368 **He X, Hu H, Wu Y, and Zeng X. 2012.** Urinary metabolites of cinobufagin in rats and their

369   antiproliferative activities. *Natural Product Research* **26(6)**:489-499. DOI

370   10.1080/14786419.2010.510798

371 **Jensen LJ, Kuhn M, Stark M, Chaffron S, Creevey C, Muller J, Doerks T, Julien P, Roth**

372   **A, Simonovic M, Bork P, and von Mering C. 2009.** STRING 8--a global view on

373   proteins and their functional interactions in 630 organisms. *Nucleic Acids Research*

374   **37**:D412-D416. DOI 10.1093/nar/gkn760

375 **Jia Q, Wang L, Zhang X, Ding Y, Li H, Yang Y, Zhang A, Li Y, Lv S, and Zhang J. 2020.**

376   Prevention and treatment of chronic heart failure through traditional Chinese medicine:

377   Role of the gut microbiota. *Pharmacological Research* **151**:104552.

378 https://doi.org/10.1016/j.phrs.2019.104552

379 **Lan Y, Wang X, Lou J-C, Xing J-S, Yu Z, Wang H, Zou S, Ma X, and Zhang B. 2018**.

380 Bufalin inhibits glioblastoma growth by promoting proteasomal degradation of the

381 Na(+)/K(+)-ATPase α1 subunit. *Biomedicine & Pharmacotherapy* **103**:204-215. DOI

382 10.1016/j.biopha.2018.04.030

383 **Laursen M, Gregersen JL, Yatime L, Nissen P, and Fedosova N. 2015**. Structures and

384 characterization of digoxin- and bufalin-bound Na+,K+-ATPase compared with the

385 ouabain-bound complex. *Proceedings of the National Academy of Sciences of the United*

386 *States of America* **112(6)**:1755-1760. DOI 10.1073/pnas.1422997112

387 **Liang Y, Liu A, Qin S, Sun J, Yang M, Li P, and Guo D. 2008.** Simultaneous determination

388 and pharmacokinetics of five bufadienolides in rat plasma after oral administration of

389 Chansu extract by SPE-HPLC method. *Journal of Pharmaceutical and Biomedical*

390 *Analysis* **46(3)**:442-448. https://doi.org/10.1016/j.jpba.2007.11.001

391 **Lother A, and Hein L. 2016.** Pharmacology of heart failure: From basic science to novel

392 therapies. *Pharmacology & Therapeutics* **166**:136-149.

393 https://doi.org/10.1016/j.pharmthera.2016.07.004

394 **Luo Z, Yu G, Chen X, Liu Y, Zhou Y, Wang G, and Shi Y. 2020.** Integrated phytochemical

395 analysis based on UHPLC-LTQ-Orbitrap and network pharmacology approaches to

396 explore the potential mechanism of Lycium ruthenicum Murr. for ameliorating

397 Alzheimer's disease. *Food & Function* **11(2)**:1362-1372. DOI 10.1039/c9fo02840d

398 **Miao X, Zheng L, Zhao Z, Su S, Zhu , Guo J, Shang E, Qian D, and Duan J. 2019.**

399   Protective Effect and Mechanism of Boswellic Acid and Myrrha Sesquiterpenes with

400   Different Proportions of Compatibility on Neuroinflammation by LPS-Induced BV2

401   Cells Combined with Network Pharmacology. *Molecules (Basel, Switzerland)*

402   **24(21)**:3946. DOI 10.3390/molecules24213946

403   **Miyashiro Y, Nishio T, and Shimada K. 2008.** Characterization of in vivo metabolites of toad

404   venom using liquid chromatography-mass spectrometry. *Journal of Chromatographic*

405   *Science* **46(6)**:534-538. DOI 10.1093/chromsci/46.6.534

406   **Molkentin J, and Robbins J. 2009.** With great power comes great responsibility: Using mouse

407   genetics to study cardiac hypertrophy and failure. *Journal of Molecular and Cellular*

408   *Cardiology* **46(2)**:130-136. https://doi.org/10.1016/j.yjmcc.2008.09.002

409   **Moreno Y, Katz A, Miklos W, Cimmino A, Tal D, Ainbinder E, Zehl M, Urban E, Evidente**

410   **A, Kopp B, Berger W, Feron O, Karlish S, and Kiss R. 2013.** Hellebrin and its

411   aglycone form hellebrigenin display similar in vitro growth inhibitory effects in cancer

412   cells and binding profiles to the alpha subunits of the Na+/K+-ATPase. *Molecular*

413   *Cancer* **12**:33. DOI 10.1186/1476-4598-12-33.

414   **Nguyen QK, Edward K, Nagasundaram N, Matthew C, and Yeh HY. 2019a.** Computational

415   identification of vesicular transport proteins from sequences using deep gated recurrent

416   units architecture. Computational and Structural Biotechnology Journal **17**:1245-1254.

417   DOI 10.1016/j.csbj.2019.09.005.

418   **Nguyen QK, Edward K, Nagasundaram N, Matthew C, and Yeh HY. 2019b.** ET-GRU:

419   using multi-layer gated recurrent units to identify electron transport proteins. BMC

420   Bioinformatics 20:377. DOI: 10.1186/s12859-019-2972-5.

421 **Ning J, Wu T, Tian Y, Wang C, Tian G, Zhang B, Liu K, and Ma X. 2010.** Identification of

422   cinobufagin metabolites in the bile of rats. *Xenobiotica* **40(1)**:48-54. DOI

423   10.3109/00498250903331049

424 **Orlov SN, Tverskoi AM, Sidorenko SV, Smolyaninova LV, Lopina OD, Dulin NO, and**

425   **Klimanova EA. 2020.** Na,K-ATPase as a target for endogenous cardiotonic steroids:

426   What's the evidence? *Genes & Diseases*. https://doi.org/10.1016/j.gendis.2020.01.008

427 **Pan Z, Luo Y, Xia Y, Zhang X, Qin Y, Liu W, Li M, Liu X, Zheng Q, and Li D. 2020.**

428   Cinobufagin induces cell cycle arrest at the S phase and promotes apoptosis in

429   nasopharyngeal carcinoma cells. *Biomedicine & Pharmacotherapy* **122**:109763.

430   https://doi.org/10.1016/j.biopha.2019.109763

431 **Qin H, Chen H, Zou Y, Zhang X, Wei C, Chen W, Xie Z, Yao M, and Han B. 2019.**

432   Systematic investigation of the mechanism of Cichorium glandulosum on type 2 diabetes

433   mellitus accompanied with non-alcoholic fatty liver rats. *Food & Function* **10(5)**:2450-

434   2460. DOI 10.1039/c8fo02284d

435 **Santulli G, and Iaccarino G. 2016.** Adrenergic signaling in heart failure and cardiovascular

436   aging. *Maturitas* **93**:65-72. https://doi.org/10.1016/j.maturitas.2016.03.022

437 **Šeflová J, Čechová P, Biler M, Hradil P, and Kubala M. 2017.** Inhibition of Na+/K+-ATPase

438   by 5,6,7,8-tetrafluoro-3-hydroxy-2-phenylquinolin-4(1H)-one. *Biochimie* **138**:56-61.

439   https://doi.org/10.1016/j.biochi.2017.04.009

440 **Shannon P, Markiel A, Ozier O, Baliga NS, Wang J, Ramage D, Amin N, Schwikowski B,**

441   **and Ideker T. 2003.** Cytoscape: a software environment for integrated models of

442   biomolecular interaction networks. *Genome Research* **13(11)**:2498-2504. DOI

443   10.1101/gr.1239303

444   **Sousa LQ, Machado KD, Oliveira SF, Araújo LD, Monção-Filho ED, Melo-Cavalcante AA,**

445   **Vieira-Júnior GM, and Ferreira PM. 2017.** Bufadienolides from amphibians: A

446   promising source of anticancer prototypes for radical innovation, apoptosis triggering and

447   Na(+)/K(+)-ATPase inhibition. *Toxicon* **127**:63-76. DOI 10.1016/j.toxicon.2017.01.004

448   **Strauss M, Smith W, Fedorova OV, and Schutte AE. 2019.** The Na(+)K(+)-ATPase Inhibitor

449   Marinobufagenin and Early Cardiovascular Risk in Humans: a Review of Recent

450   Evidence. *Current Hypertension Reports* **21(5)**:38. DOI 10.1007/s11906-019-0942-y

451   **Tao J, Mao L, Zhou B, Liu Q, Yang A, Wei G, Liu R, Zhang W, Xu W, and Ye J. 2017**.

452   Simultaneous determination of ginsenosides and bufadienolides in rat plasma after the

453   oral administration of Shexiang Baoxin Pill for pharmacokinetic study by liquid

454   chromatography tandem mass spectrometry following solid-phase extraction. *Biomedical*

455   *chromatography* **31(3)**. DOI 10.1002/bmc.3816

456   **Wang Z, Sun L, and Heinbockel T. 2014.** Resibufogenin and cinobufagin activate central

457   neurons through an ouabain-like action. *Plos One* **9(11)**:e113272. DOI

458   10.1371/journal.pone.0113272

459   **Wei W, An Y, Zhang Y, Li Z, Zhou Y, Lei M, Zhang J, Qu H, Da J, Wu W, and Guo D.**

460   **2020.** Quantitative analysis of fourteen bufadienolides in Venenum Bufonis crude drug

461   and its Chinese patent medicines by ultra-high performance liquid chromatography

462   coupled with tandem mass spectrometry. *Journal of Ethnopharmacology* **251**:112490.

463   https://doi.org/10.1016/j.jep.2019.112490

464   **Wei W, Hou J, Wang X, Yu Y, Li H, Li Z, Feng Z, Qu H, Wu W, and Guo D. 2019.**

465   Venenum bufonis: An overview of its traditional use, natural product chemistry,

466   pharmacology, pharmacokinetics and toxicology. *Journal of Ethnopharmacology*

467   **237**:215-235. https://doi.org/10.1016/j.jep.2019.03.042

468   **Wu S, Hsiao Y, Kuo C, Yu F, Hsu S, Wu P, Chen J, Hsia T, Liu H, Hsu W, and Chung J.**

469   **2015.** Bufalin Inhibits NCI-H460 Human Lung Cancer Cell Metastasis In Vitro by

470   Inhibiting MAPKs, MMPs, and NF-κB Pathways. *The American journal of Chinese*

471   *medicine* **43(6)**:1247-1264. DOI 10.1142/s0192415x15500718

472   **Xia X, Jin H, Yan S, and Zhang W. 2010.** Analysis of the bioactive constituents of ChanSu in

473   rat plasma by high performance liquid chromatography with mass spectrometric

474   detection. *Journal of Pharmaceutical and Biomedical Analysis* **53(3)**:646-654. DOI

475   10.1016/j.jpba.2010.05.009

476   **Xin X, Dong P, Sun X, Deng S, Zhang N, Wang C, Huo X, Li Y, Lan R, Chen L, and Fan**

477   **G. 2016.** Identification of the hydroxylated derivatives of bufalin: phase I metabolites in

478   rats. *Journal of Asian Natural Products Research* **18(3)**:239-247. DOI

479   10.1080/10286020.2015.1071358

480   **Xu S, Wang Y, Yu M, Wang D, Liang Y, Chen Y, Liao C, Xie Z, Zhao B, Han J, Duan Y,**

481   **and Yang X. 2020.** LongShengZhi capsule inhibits doxorubicin-induced heart failure by

482   anti-oxidative stress. *Biomedicine & Pharmacotherapy* **123**:109803.

483   https://doi.org/10.1016/j.biopha.2019.109803

484   **Yang L, Li A, Chen M, Yan Y, Liu Y, Li K, Jia J, and Qin X. 2020.** Comprehensive

485   investigation of mechanism and effective ingredients of Fangji Huangqi Tang by serum

486   pharmacochemistry and network pharmacology. *Biomedical chromatography*

487   **34(4)**:e4785. DOI 10.1002/bmc.4785

488   **Yang Y, Shi C, Xie J, Dai J, He S, Tian Y. 2020.** Identification of Potential Dipeptidyl

489   Peptidase (DPP)-IV Inhibitors among Moringa oleifera Phytochemicals by Virtual

490   Screening, Molecular Docking Analysis, ADME/T-Based Prediction, and In Vitro

491   Analyses. Molecules **25(1)**:189. DOI: 10.3390/molecules25010189.

492   **Yu G, Luo Z, Zhou Y, Zhang L, Wu Y, Ding L, and Shi Y. 2019.** Uncovering the

493   pharmacological mechanism of Carthamus tinctorius L. on cardiovascular disease by a

494   systems pharmacology approach. *Biomedicine & Pharmacotherapy* **117**:109094.

495   https://doi.org/10.1016/j.biopha.2019.109094

496   **Yu G, Wang W, Wang X, Xu M, Zhang L, Ding L, Guo R, and Shi Y. 2018.** Network

497   pharmacology-based strategy to investigate pharmacological mechanisms of Zuojinwan

498   for treatment of gastritis. *BMC Complementary and Alternative Medicine* **18(1)**:292-292.

499   DOI 10.1186/s12906-018-2356-9

500   **Yu G, Zhang Y, Ren W, Dong L, Li J, Geng Y, Zhang Y, Li D, Xu H, and Yang H. 2016.**

501   Network pharmacology-based identification of key pharmacological pathways of Yin-

502   Huang-Qing-Fei capsule acting on chronic bronchitis. *International Journal of Chronic*

503   *Obstructive Pulmonary Disease* **12**:85-94. DOI 10.2147/COPD.S121079

504   **Yun HR, Yoo HS, Shin DY, Hong SH, Kim J-H, Cho CK, and Choi YH. 2009.** Apoptosis

505   Induction of Human Lung Carcinoma Cells by Chan Su (Venenum Bufonis) Through

506   Activation of Caspases. *Journal of Acupuncture and Meridian Studies* **2(3)**:210-217.

507   https://doi.org/10.1016/S2005-2901(09)60057-1

508   **Zhang X, Pi Z, Zheng Z, Liu Z, and Song F. 2018.** Comprehensive investigation of in-vivo

509   ingredients and action mechanism of iridoid extract from Gardeniae Fructus by liquid

510   chromatography combined with mass spectrometry, microdialysis sampling and network

511   pharmacology. *Journal of Chromatography B* **1076**:70-76.

512   https://doi.org/10.1016/j.jchromb.2018.01.023

513   **Zhang Z, Yi P, Yang J, Huang J, Xu P, Hu M, Zhang C, Wang B, and Peng W. 2020.**

514   Integrated network pharmacology analysis and serum metabolomics to reveal the

515   cognitive improvement effect of Bushen Tiansui formula on Alzheimer's disease. *Journal*

516   *of Ethnopharmacology* **249**:112371. https://doi.org/10.1016/j.jep.2019.112371

517   **Zhu Z, Deng S, Liu D, Zhang BJ, Sun HZ, Tian Y, Wang CY, Wang L, and Ma X. 2013.**

518   Isolation and identification of phase I metabolites of resibufogenin in rats. *Xenobiotica*

519   **43(5)**:479-485. DOI 10.3109/00498254.2012.728728

520

521   **Figure Captions**

522   **Fig. 1.** Workflow of network pharmacology and molecular docking approaches to reveal the

523   active components and molecular mechanisms of VB acting on HF.

524   **Fig. 2.** GO term performance and pathway enrichment analysis of the major hubs. (a) GO: BP;

525 (b) GO: MF; (c) GO: CC; and (d) KEGG. The ordinate stands for GO terms or the main

526 pathways, the primary abscissa stands for minus log 10(P), and the secondary abscissa stands for

527 the percentage of major hubs involved in the corresponding GO terms or the main pathways out

528 of total major hubs.

529 **Fig. 3.** VB ingredients-major hubs-pathway network.

530 Green V-diagrams represent each prototype component in VB; yellow V-diagrams represent

531 each metabolite in VB; round blue nodes represent putative targets of components in VB; round

532 red nodes represent known therapeutic targets for HF; orange rectangles represent top 11

533 pathways from enrichment analysis of major targets; edges represent interactions among VB

534 ingredients, putative targets, known therapeutic targets for the treatment of VB, and main

535 pathways.

536 **Fig. 4.** Adrenergic signalling in cardio-myocytes influenced by major putative targets of VB

537 components.

538 **Fig. 5.** The binding modes of the selected compounds and targets.

539 (a) Schematic (3D) representation and (b) Schematic (2D) representation of the interplay

540 between bufotalin and ATP1A1 (PDB IDchimeric 3N23).

541 (c) Schematic (3D) representation and (d) Schematic (2D) representation of the interplay

542 between cinobufaginol and GNAS (PDB IDchimeric 3C14).

543 (e) Schematic (3D) representation and (f) Schematic (2D) representation of the interplay between

544 cinobufaginol and MAPK1 (PDB IDchimeric 3O71).

545 (g) Schematic (3D) representation and (h) Schematic (2D) representation of the interplay

546   between 19-oxo-bufalin and PRKCA (PDB IDchimeric 4DNL).

547   Active site amino acid residues were represented as tubes, while the compounds were shown as

548   stick model with purple colored.

Molecular docking results (Top 5 for each targets)

1 **Table 1**

2 Molecular docking results (Top 5 for each targets).

Targets	Compound	-CIE (kcal/mol)
ATP1A1	Bufotalin	49.0335
	Cinobufotalin	46.109
	Cinobufagin	45.1269
	Cinobufaginol	44.0494
	5β, 6α-dihydroxybufalin	43.3908
GNAS	Cinobufaginol	55.2668
	6α-hydroxybufalin	53.1182
	19-oxo-desacetylcinobufagin	52.2151
	1,5-dihydroxyldesacetylcinobufagin	49.9538
	1,12β-dihydroxycinobufagin	49.4652
MAPK1	Cinobufaginol	55.1432
	Cinobufagin	54.0654
	Bufotalin	53.1891
	1,5-dihydroxyldesacetylcinobufagin	51.5985
	12-hydroxyl-cinobufagin	51.2183
PRKCA	19-oxo-bufalin	42.0454
	Marinobufagin	39.3428

Hellebrigenin	38.6171
5β, 6α-dihydroxybufalin	37.9654
Resibufogenin	37.8932

Figure 1

Workflow of network pharmacology and molecular docking approaches to reveal the active components and molecular mechanisms of VB acting on HF

Venenum Bufonis (VB)   **In vivo constituents of VB**   **Targets of VB**   **Network analysis**

PPI

Heart Failure   **Disease associated databases**   **Disease associated genes**   **GO&KEGG analysis**

Molecular docking   **Core pathway**   **Chemical-Target-Pathway network**

- **Mechanism clarification**
- **Molecular validation**
- **Drug discovery**
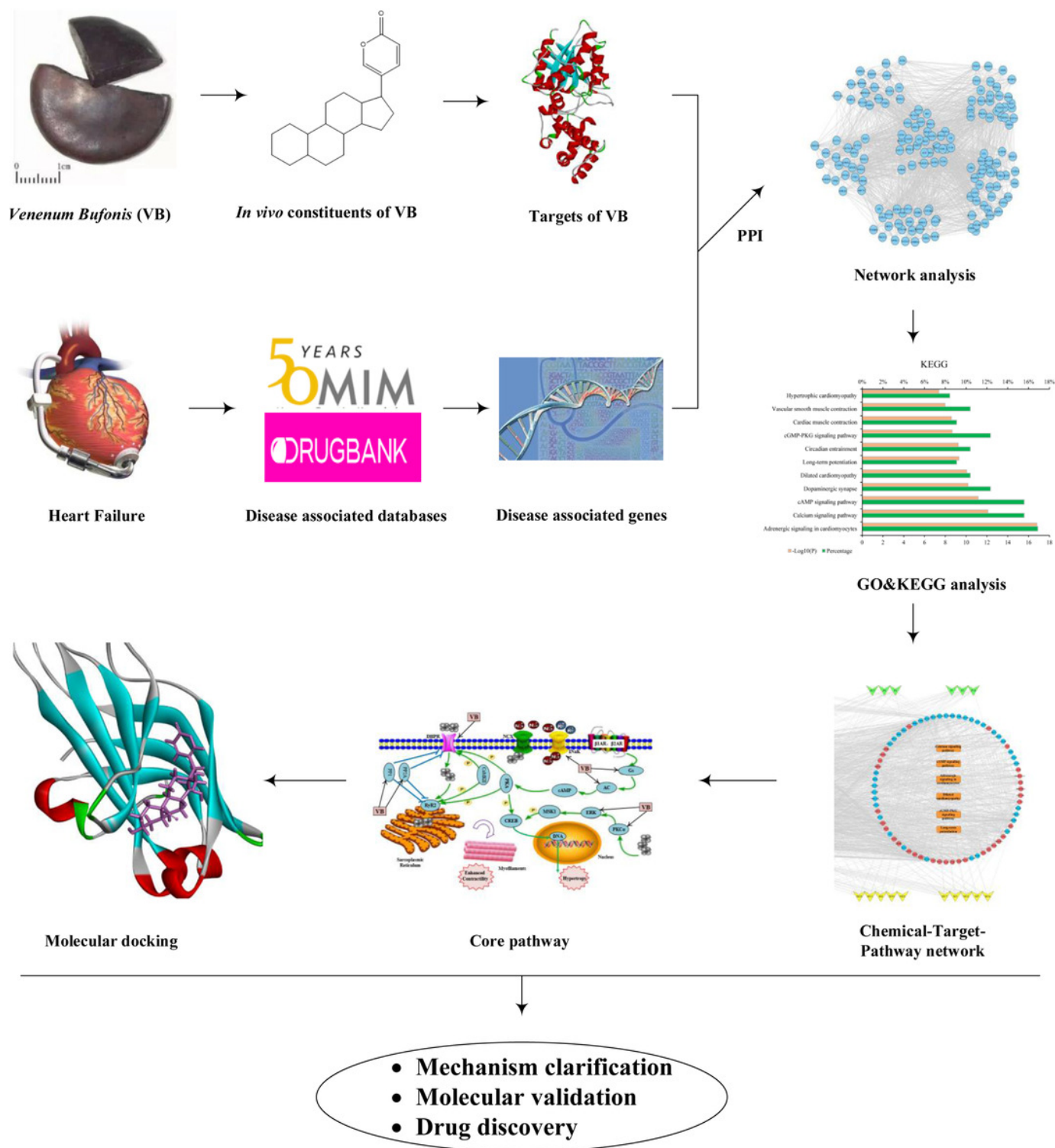
Figure 2

GO term performance and pathway enrichment analysis of the major hubs.

(a) GO: BP; (b) GO: MF; (c) GO: CC; and (d) KEGG. The ordinate stands for GO terms or the main pathways, the primary abscissa stands for minus log 10(P), and the secondary abscissa stands for the percentage of major hubs involved in the corresponding GO terms or the main pathways out of total major hubs.
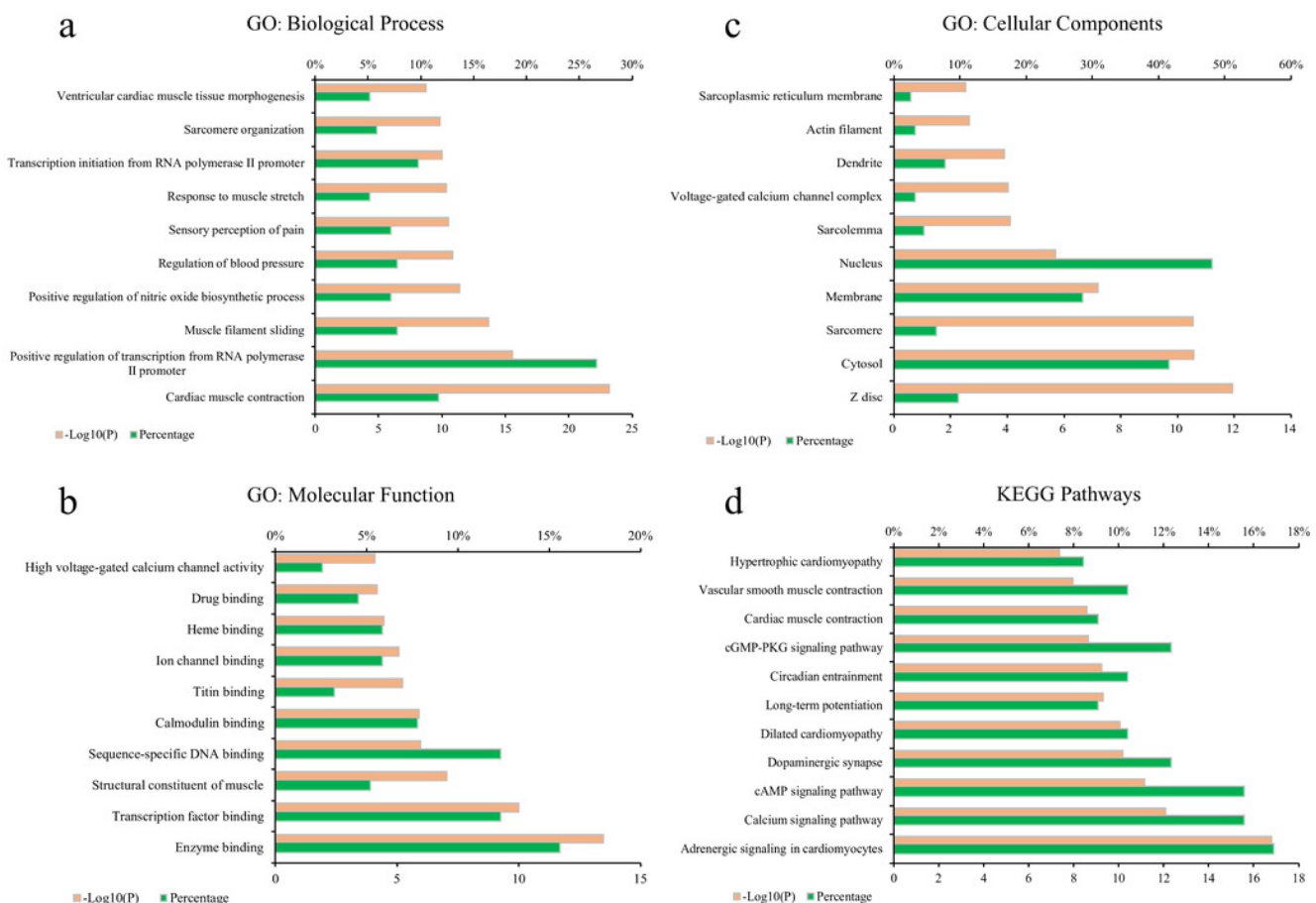
Figure 3

VB ingredients-major hubs-pathway network.

Green V-diagrams represent each prototype component in VB; yellow V-diagrams represent each metabolite in VB; round blue nodes represent putative targets of components in VB; round red nodes represent known therapeutic targets for HF; orange rectangles represent top 11 pathways from enrichment analysis of major targets; edges represent interactions among VB ingredients, putative targets, known therapeutic targets for the treatment of VB, and main pathways.
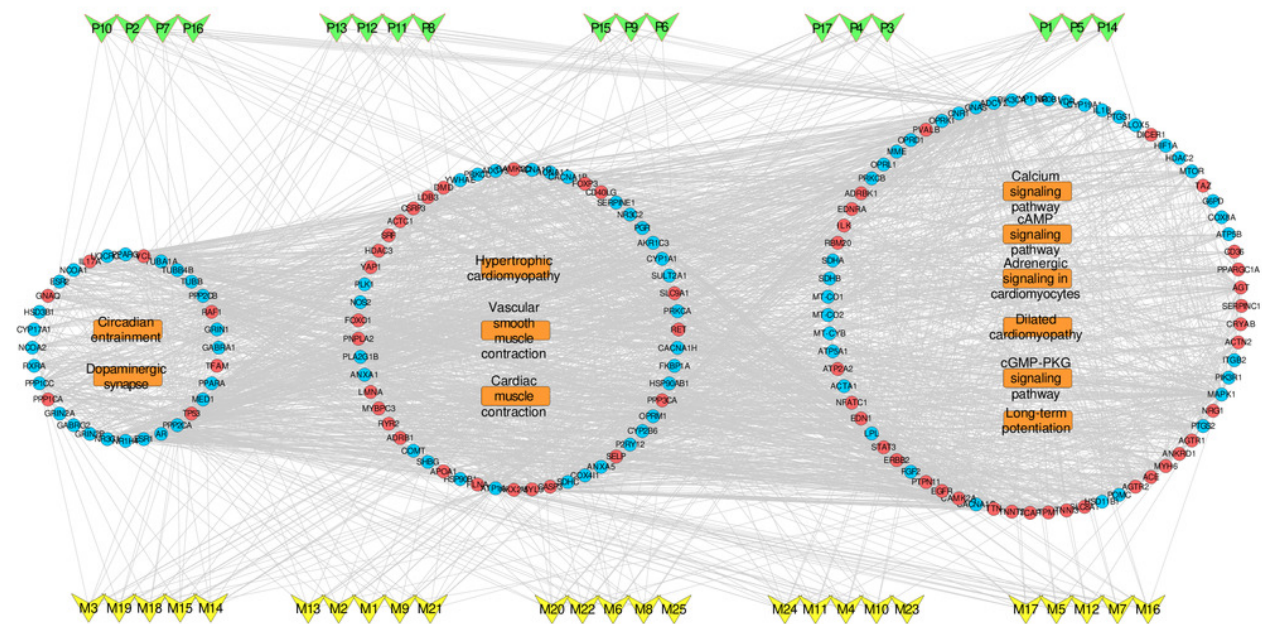
Figure 4

Adrenergic signalling in cardio-myocytes influenced by major putative targets of VB components.
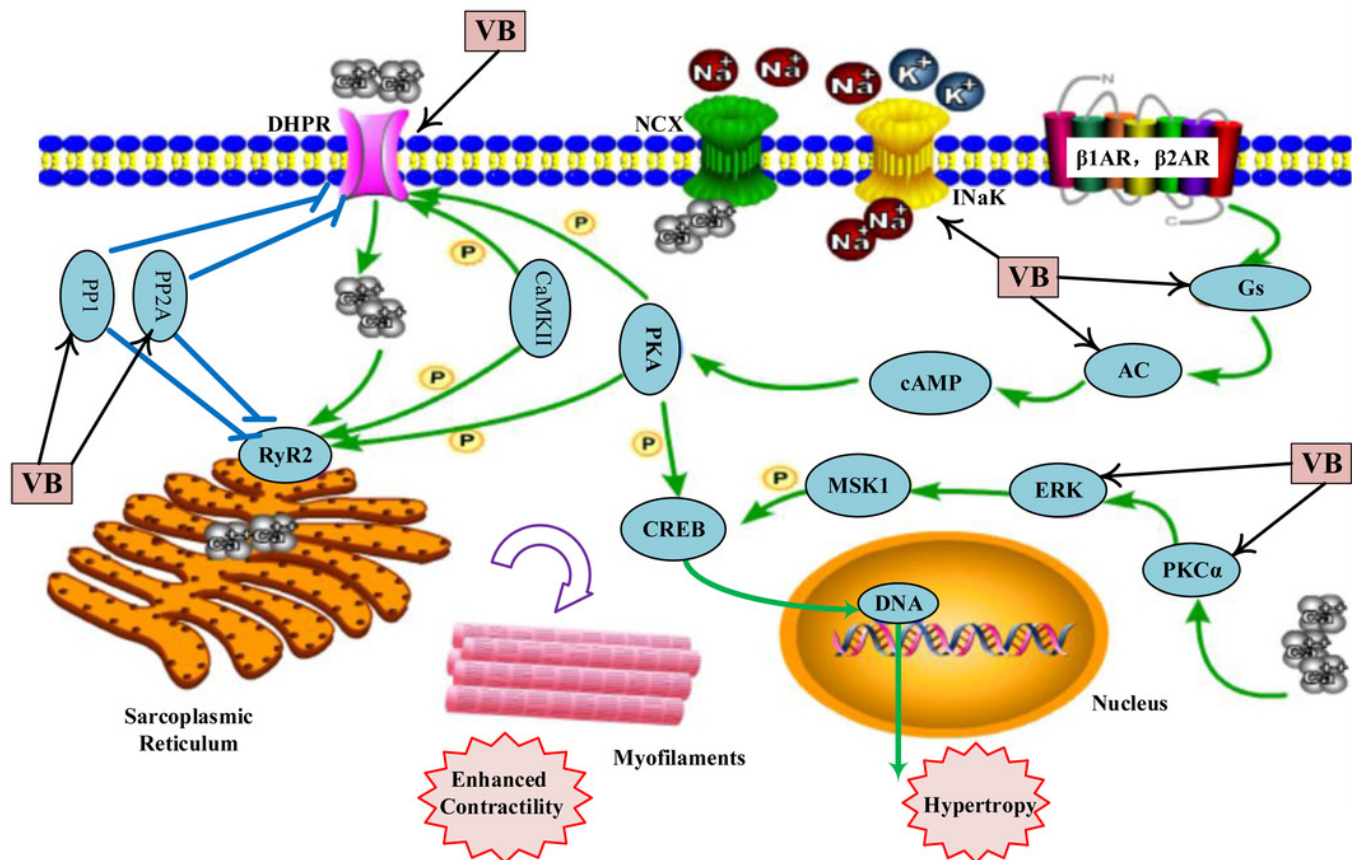
Figure 5

The binding modes of the selected compounds and targets.

(a) Schematic (3D) representation and (b) Schematic (2D) representation of the interplay between bufotalin and ATP1A1 (PDB IDchimeric 3N23). (c) Schematic (3D) representation and (d) Schematic (2D) representation of the interplay between cinobufaginol and GNAS (PDB IDchimeric 3C14). (e) Schematic (3D) representation and (f) Schematic (2D) representation of the interplay between cinobufaginol and MAPK1 (PDB IDchimeric 3O71). (g) Schematic (3D) representation and (h) Schematic (2D) representation of the interplay between 19-oxo-bufalin and PRKCA (PDB IDchimeric 4DNL). Active site amino acid residues were represented as tubes, while the compounds were shown as stick model with purple colored.

a

c

b

MET
A:157
GLY   ASP
A:731   A:733
ASP   PHE
A:710   ALA   SER   A:258
         A:730 A:732
GLY   LEU
A:711   A:173

H
SER   VAL VAL MET
A:209   SER A:260 A:734 A:260
         SER   A:191   ALA
ASN   A:210 ASN ARG   A:264
A:377   A:241 THR
                      A:240

Interactions
- ☐ van der Waals
- ☐ Conventional Hydrogen Bond
- ☐ Carbon Hydrogen Bond
- ☐ Alkyl

d

LEU
C:296
SER   GLU   SER
C:252   C:299   C:306
ASP
C:173
ILE   H
C:172 LEU
       C:171
              ASN SER GLN   GLU LYS
              C:167 C:166 C:176 C:164 C:305
       MET   TYR   ALA
       C:255 ASN   C:163 C:303
              C:254

Interactions
- ☐ van der Waals
- ☐ Conventional Hydrogen Bond
- ☐ Carbon Hydrogen Bond
- ☐ Pi-Cation
- ☐ Pi-Anion
- ☐ Alkyl
- ☐ Pi-Alkyl

e

g

f

ALA   CYS
A:187   A:164
VAL   LYS   ASN   LYS
A:186 A:149 A:152 A:52 SER
                        A:151 GLN
                               A:103
ARG
A:65
       H   H   LEU
                               A:154
   ALA   GLY
TYR A:33 A:32
A:34 ASP   GLU VAL GLY   THR
      A:165 A:37 A:30 ASP   A:108
               ILE A:109 LYS
               A:29   A:112

Interactions
- ☐ van der Waals
- ☐ Conventional Hydrogen Bond
- ☐ Carbon Hydrogen Bond
- ☐ Pi-Anion
- ☐ Alkyl
- ☐ Pi-Alkyl

h

LEU
A:231
THR   LYS   ASP   LEU
A:228 PHE A:230   A:235 A:200
       A:229
GLN   ARG
A:210   A:238
              H
       LYS
SER   A:232   PRO
A:208 GLU   ASP   A:202
LYS   A:207 A:203
A:209   LYS   PRO
              A:205 A:204

Interactions
- ☐ van der Waals
- ☐ Conventional Hydrogen Bond
- ☐ Alkyl